

iScience, Volume 27

Supplemental information

CCRR regulate MYZAP-PKP2-Nav1.5

signaling pathway in atrial fibrillation

following myocardial infarction

Lina Xuan, Jianjun Guo, Huishan Luo, Shijia Cui, Feihan Sun, Guangze Wang, Xingmei Yang, Siyun Li, Hailong Zhang, Qingqing Zhang, Hua Yang, Shengjie Wang, Xiaolin Hu, Baofeng Yang, and Lihua Sun

Figure S1

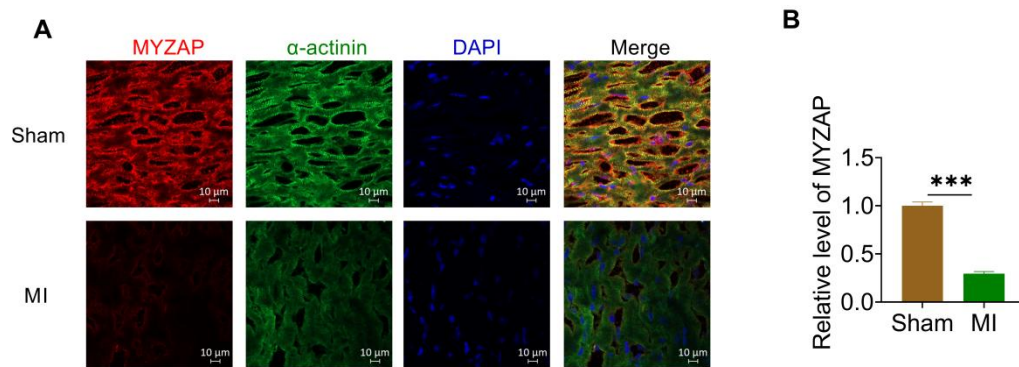


Figure S1. Decreased expression of MYZAP in mouse atria after myocardial infarction. Related to Figure 1.

Immunofluorescence results showed that the expression level of MYZAP in atrial tissue was decreased 12 h after MI in mice (Sham $n = 40$, MI $n = 23$ visions). Red represents MYZAP, green represents α -actinin, and blue represents nucleus. Data are presented as mean \pm SEM. *** $P < 0.001$ (unpaired t -test).

Figure S2

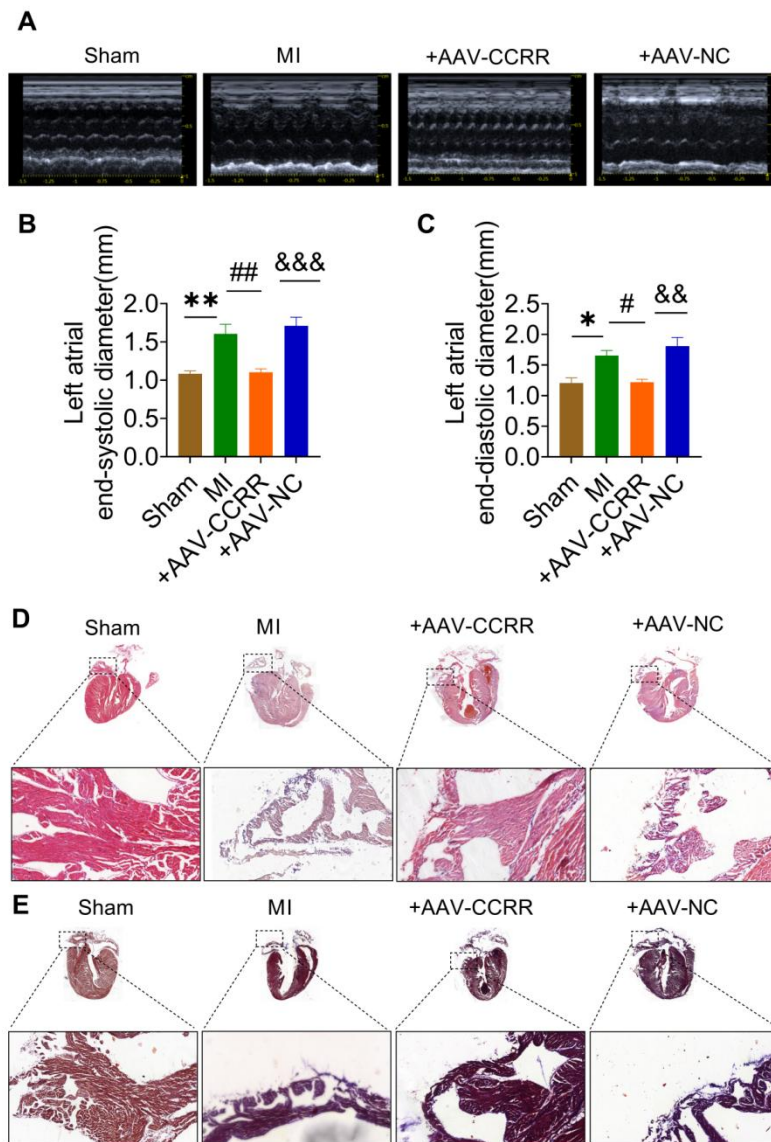


Figure S2. CCRR reverses atrial damage after myocardial infarction. Related to Figure 2.

(A) Representing echocardiogram of mouse atrium. (B-C) After MI, the left atrial diameter was increased at the end of atrial systole and end of diastole, and CCRR effectively reversed the increased atrial diameter (Sham, +AAV-NC $n = 8$, MI $n = 7$, +AAV-CCRR $n = 6$ mice/group). (D) HE staining showed that 12 h after MI, atrial cardiomyocytes were disordered and observed infiltration of inflammatory cells ($n = 3$ mice/group). (E) Masson staining did not show significant atrial fibrosis ($n = 3$ mice/group). Data are presented as mean \pm SEM. $*P < 0.05$, $**P < 0.01$. $\#P < 0.05$, and $\#\#P < 0.01$. $\&\&P < 0.01$, and $\&\&\&P < 0.001$ (One-way ANOVA).

Figure S3


RNA-Protein Interaction Prediction (RPISeq)

Dobbs and Honavar Laboratories

- Home
- About/FAQs
- Datasets
- Related Links
- References
- Funding
- Contact Us

Links

- Dobbs Lab Software
- Bioinformatics and Computational Biology
- Center for Computational Intelligence, Learning & Discovery
- Department of Genetics, Development and Cell Biology



Welcome to RPISeq

Submit a protein sequence and an RNA sequence to predict the interaction probability.

Enter **Protein** Sequence in *PLAIN TEXT* format: [sample](#)

```
CTTGGAATTTAATAATTTAGTGTCTCAGTATCAATTGGTGTGTTTTGTTAAACGAAT
GAATCATCTGTT
CATGCATGCTCTACTTTGATATTATAACCTATGTCACATGTGTTAATAAATACCATAT
ATTTTGTCTA
CTAA
```

Enter **RNA** Sequence in *PLAIN TEXT* format: [sample](#)

```
TCCTACTGCATAT
GCCTAGCTACATTGAGCTAGCTTTCACCTTCATGGTGGTGGGGCTGAGGCTAGCAG
GCACAGAGGAGTAG
ACCAGCAGCTGAGAGCTTATGCTATAACCCC
```

To run RPISeq for a single protein and multiple RNA sequences, click [here](#).

To run RPISeq for a single RNA and multiple protein sequences, click [here](#).

Interaction probabilities

Prediction using RF classifier 0.8

Prediction using SVM classifier 0.82

Figure S3. Theoretical prediction of the interaction between CCRR and MYZAP.

Related to Figure 3.

Theoretical analysis of RNA: protein binding using the RNA-Protein Interaction Prediction (RPISeq) database, which revealed a high probability of CCRR : MYZAP interaction.

Figure S4

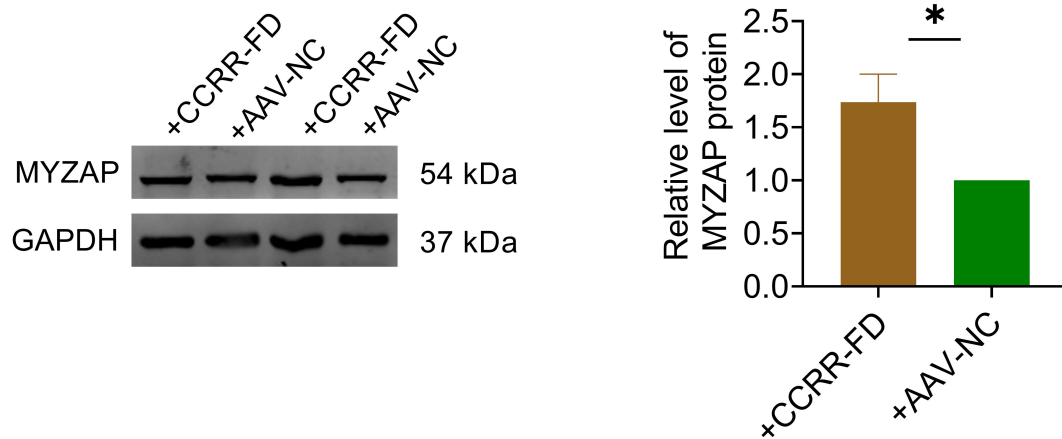


Figure S4. CCRR-Functional domain (CCRR-FD) reverses the down-regulation of MYZAP expression in atrial tissue after MI. Related to Figure 3.

AAV-CCRR-FD virus was constructed and injected into the tail vein for 4 weeks. +AAV-NC: MI+AAV-NC, +CCRR-FD: MI+CCRR-FD. Compared with +AAV-NC group, +CCRR-FD overexpression significantly up-regulated the expression of MYZAP in atrial tissue 12 h after MI in mice ($n = 5$ mice/group). Data are presented as mean \pm SEM. * $P < 0.05$ (unpaired t -test).

Figure S5

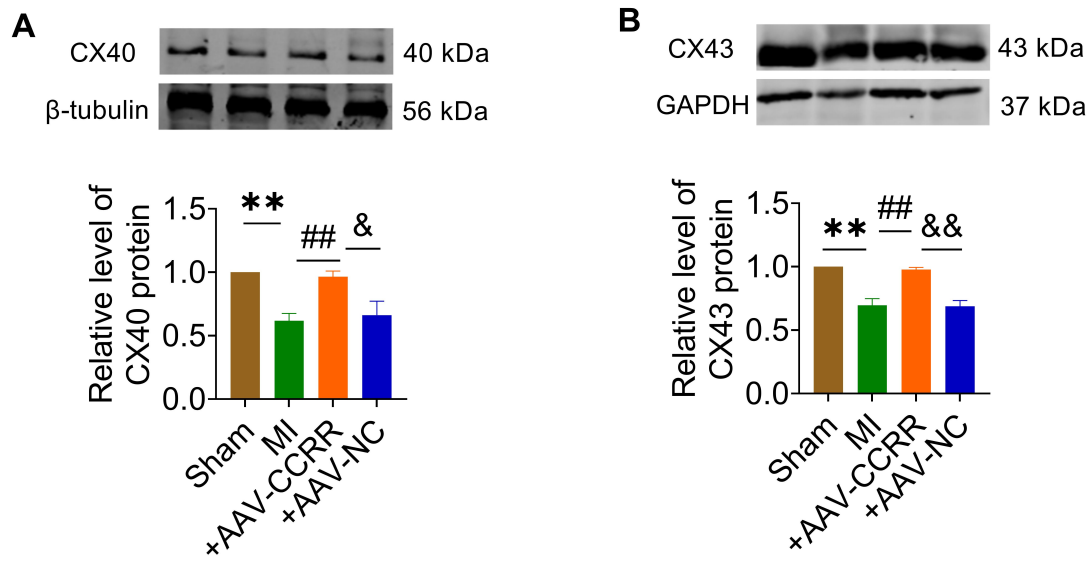


Figure S5. CCRR regulates the expression of CX40 and CX43 in atrial tissue after myocardial infarction. Related to Figure 3.

Compared with the sham group, the expression of CX40 and CX43 in atrial tissue was decreased significantly 12h after MI. However, the expression levels of CX40 and CX43 were restored after the overexpression of AAV-CCRR (A, $n = 5/\text{group}$, B, $n = 3/\text{group}$). Data are presented as mean \pm SEM. ** $P < 0.01$. ## $P < 0.01$. & $P < 0.05$, and && $P < 0.01$ (One-way ANOVA).

Figure S6

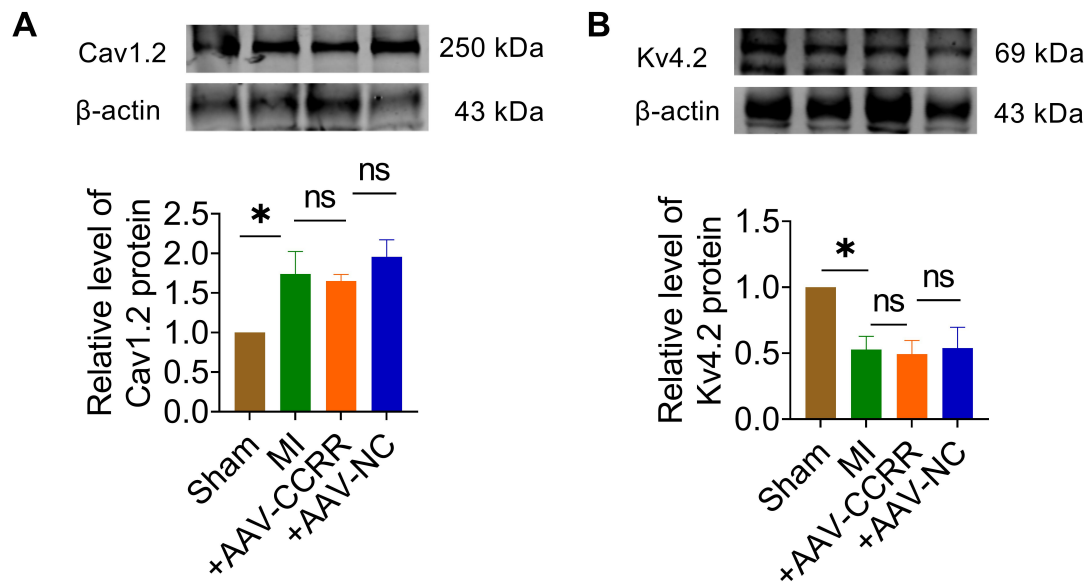


Figure S6. CCRR had no regulatory effect on the expression levels of Cav1.2 and Kv4.2. Related to Figure 3.

(A-B) Western blot results indicated that 12 h after MI, the expression of Cav1.2 was increased in atrial tissues, while the expression of Kv4.2 was decreased. The AAV-CCRR treatment group showed no significant regulatory effect (A, $n = 6/\text{group}$, B, $n = 4/\text{group}$). Data are presented as mean \pm SEM. $*P < 0.05$, and $ns > 0.05$. (One-way ANOVA).

Figure S7

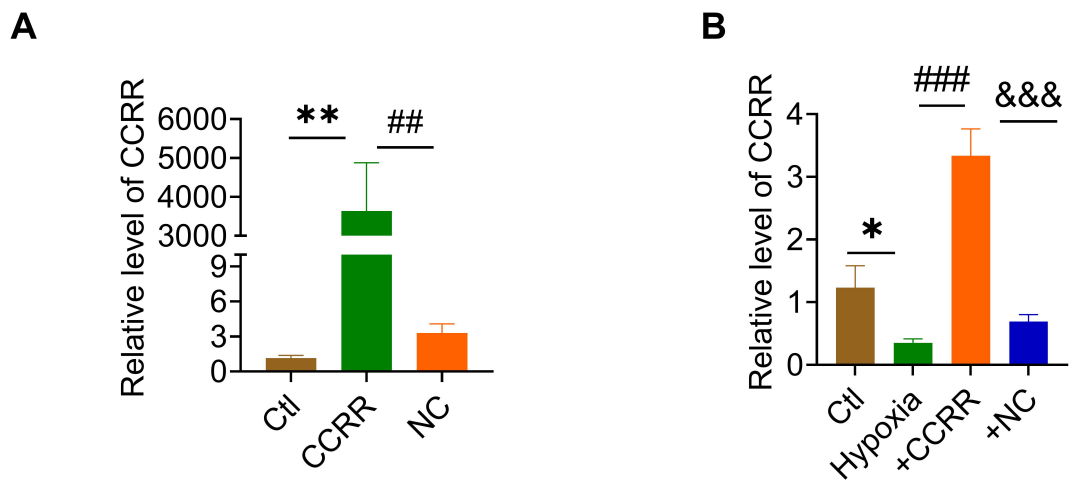


Figure S7. Verification of CCRR overexpression plasmid efficiency. Related to Figure 3.

(A) Real-time PCR results showed that compared with NC group, the expression level of CCRR in CCRR plasmid group was significantly increased ($n = 6/\text{group}$). (B) Compared with Ctl group, the expression level of CCRR in atrial myocytes decreased after hypoxia. Overexpression of CCRR can be significantly restored ($n = 6/\text{group}$). Data are presented as mean \pm SEM. $*P < 0.05$, $**P < 0.01$. $##P < 0.01$, and $###P < 0.001$. $\&\&\&P < 0.001$ (One-way ANOVA).

Figure S8

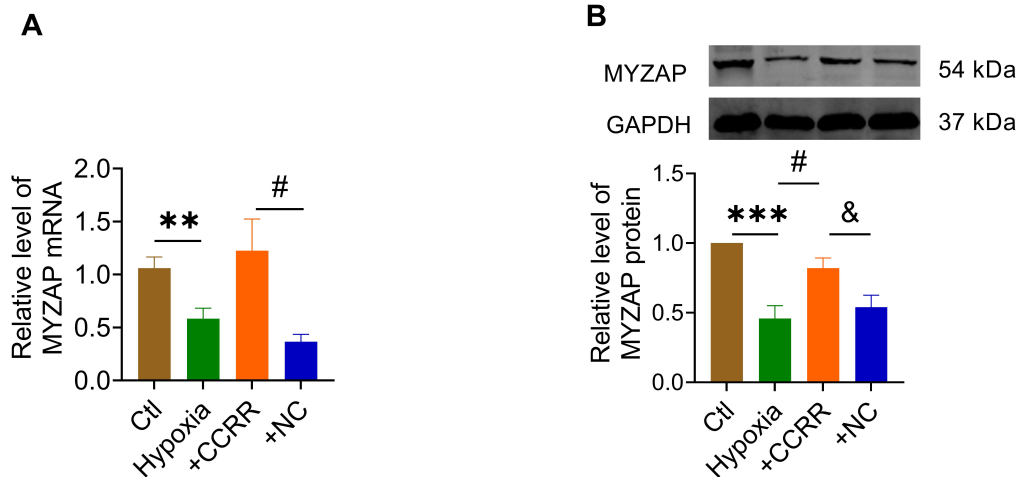


Figure S8. Overexpression of CCRR reverses the decreased expression of MYZAP after hypoxia. Related to Figure 3.

(A) Real-time PCR was used to detect the expression of MYZAP mRNA in atrial cardiomyocytes ($n = 9/\text{group}$). (B) Western blot was used to detect the expression of MYZAP protein in atrial cardiomyocytes. Compared with Ctl group, the expression of MYZAP protein was decreased significantly after hypoxia. The expression of MYZAP was significantly restored by overexpression of CCRR compared with NC group ($n = 5/\text{group}$). Data are presented as mean \pm SEM. $**P < 0.01$, and $***P < 0.001$. $\#P < 0.05$. $\&P < 0.05$ (One-way ANOVA).

Figure S9

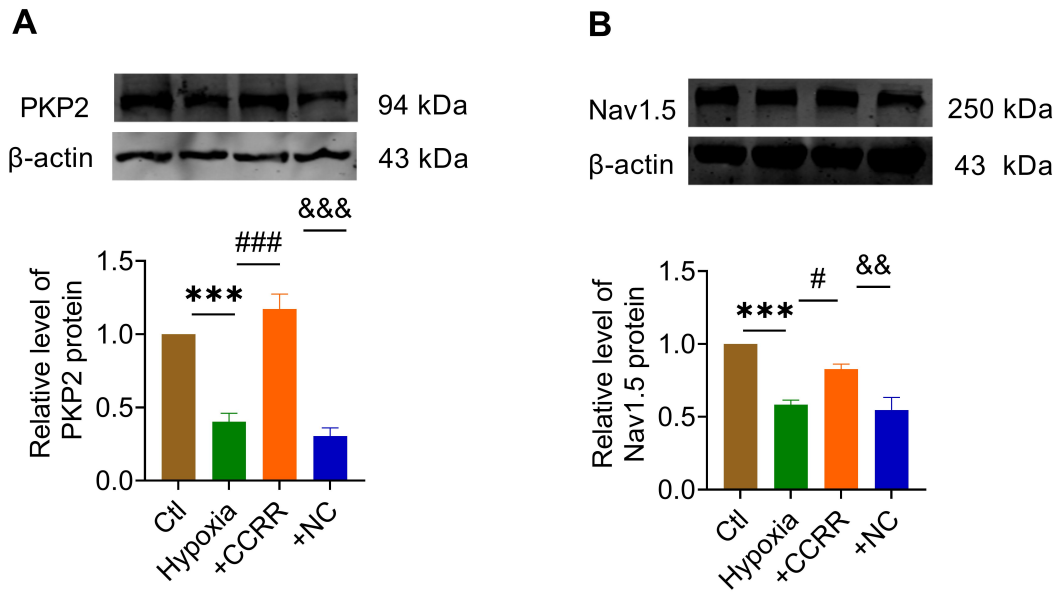


Figure S9. CCRR may act as an upstream regulator to regulate the expression of PKP2 and Nav1.5. Related to Figure 3.

(A-B) Western blot were used to detect the expression of PKP2 and Nav1.5 protein in atrial cardiomyocytes. Compared with Ctl group, the protein expression of PKP2 and Nav1.5 was decreased significantly after hypoxia. The expression of PKP2 and Nav1.5 was significantly restored by CCRR (A, $n = 6$ /group. B, $n = 4$ /group). Data are presented as mean \pm SEM. *** $P < 0.001$. # $P < 0.05$, and ### $P < 0.001$. && $P < 0.01$, and &&& $P < 0.001$ (One-way ANOVA).

Figure S10

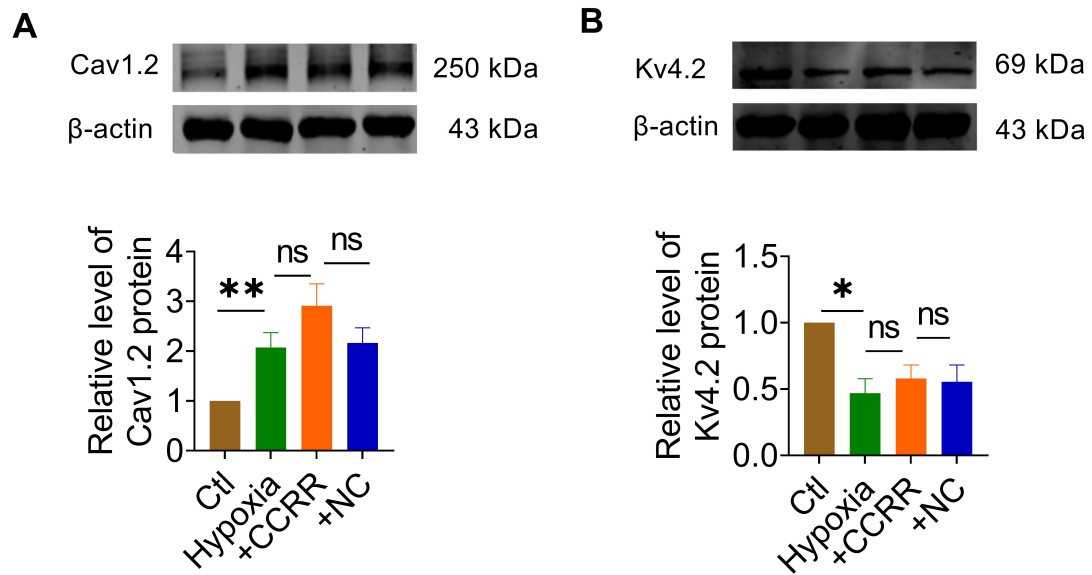


Figure S10. CCRR did not significantly regulate the expression levels of Cav1.2 and Kv4.2 in hypoxic atrial myocytes. Related to Figure 3.

(A-B) After 12h of hypoxia, the expression of Cav1.2 protein was increased, while Kv4.2 protein was decreased in primary atrial cardiomyocytes. Overexpression of CCRR had no reverse effect (A, $n = 6/\text{group}$, B, $n = 3/\text{group}$). Data are presented as mean \pm SEM. * $P < 0.05$, ** $P < 0.01$ and $ns > 0.05$. (One-way ANOVA).

Figure S11

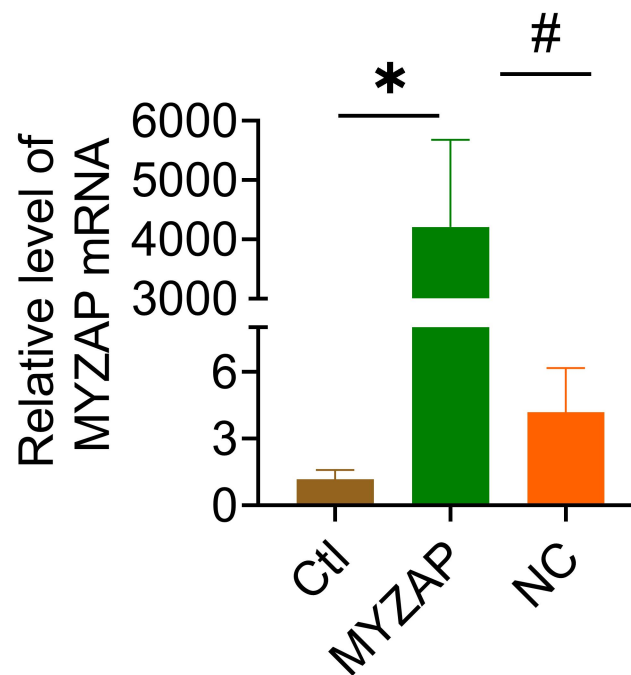


Figure S11. Validation of MYZAP overexpression plasmid efficiency. Related to Figure 4.

MYZAP overexpression plasmid was transfected into atrial cardiomyocytes, and the expression efficiency of the plasmid was verified by Real-time PCR ($n = 9/\text{group}$).

Data are presented as mean \pm SEM. * $P < 0.05$; # $P < 0.05$ (One-way ANOVA).

Figure S12

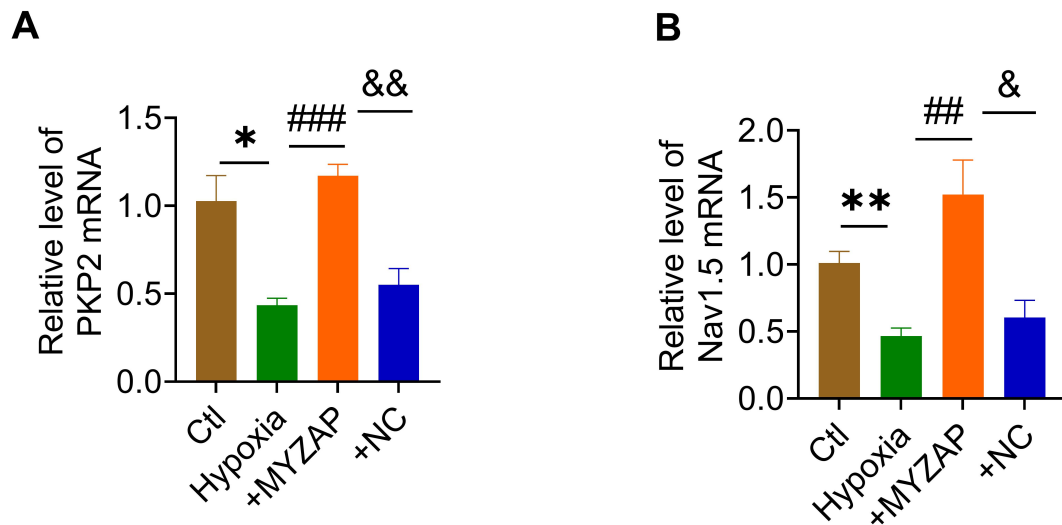


Figure S12. Overexpression of MYZAP reverses hypoxia-induced mRNA downregulation of PKP2 and Nav1.5. Related to Figure 4.

(A) Compared with Ctl group, the expression of PKP2 mRNA decreased after 12h of hypoxia in atrial myocardium. Compared with hypoxia+NC group, the mRNA expression of PKP2 was significantly up-regulated in hypoxia+MYZAP group ($n = 4/\text{group}$). (B) Compared with Ctl group, Nav1.5 mRNA expression was decreased after 12h of hypoxia. Compared with hypoxia+NC group, the mRNA expression level of Nav1.5 was significantly upregulated in hypoxia+MYZAP group (Ctl, Hypoxia $n = 4$. +MYZAP, +NC $n = 3$). Data are presented as mean \pm SEM. $*P < 0.05$, $**P < 0.01$. $###P < 0.01$, $####P < 0.001$. $\&P < 0.05$, $\&\&P < 0.01$ (One-way ANOVA).

Figure S13

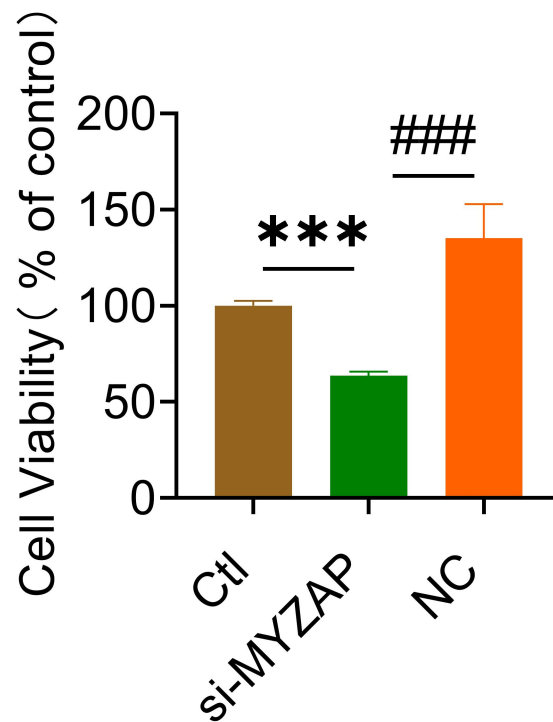


Figure S13. Loss of MYZAP correlates with cell viability. Related to Figure 4.

Compared with NC group, the viability of atrial myocytes transfected with si-MYZAP was significantly decreased ($n = 9/\text{group}$). Data are presented as mean \pm SEM. *** $P < 0.001$. ### $P < 0.001$ (One-way ANOVA).

Figure S14

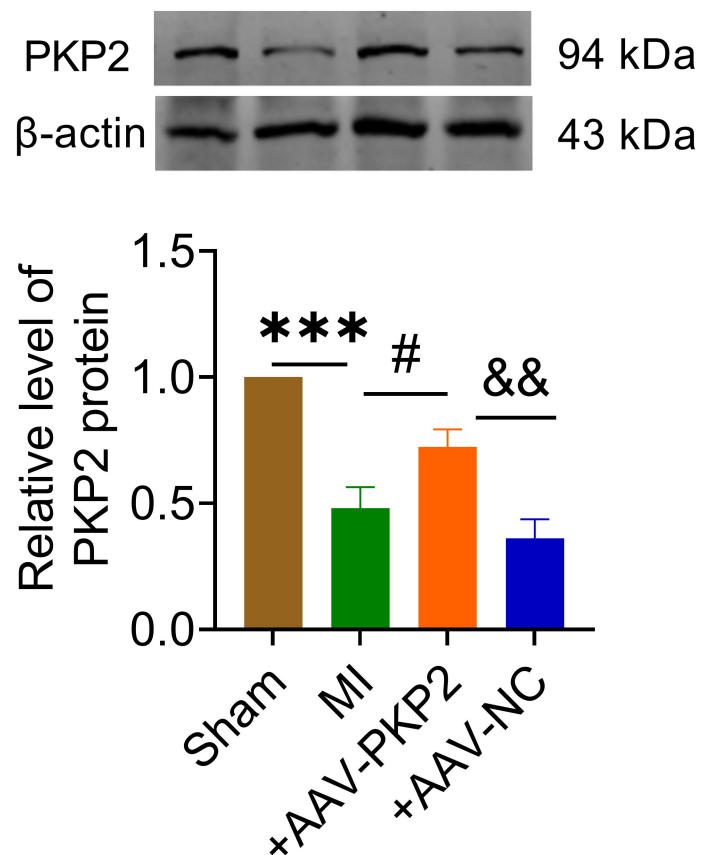


Figure S14. Efficiency verification of overexpressing AAV-PKP2 virus. Related to Figure 5.

PKP2 expression was down-regulated in atrial tissue after myocardial infarction, and PKP2 overexpressing could restore the expression level of PKP2 in atrium after tail vein injection of AAV-PKP2 virus ($n = 5/\text{group}$). Data are presented as mean \pm SEM. *** $P < 0.001$. # $P < 0.05$. && $P < 0.01$ (One-way ANOVA).

Figure S15

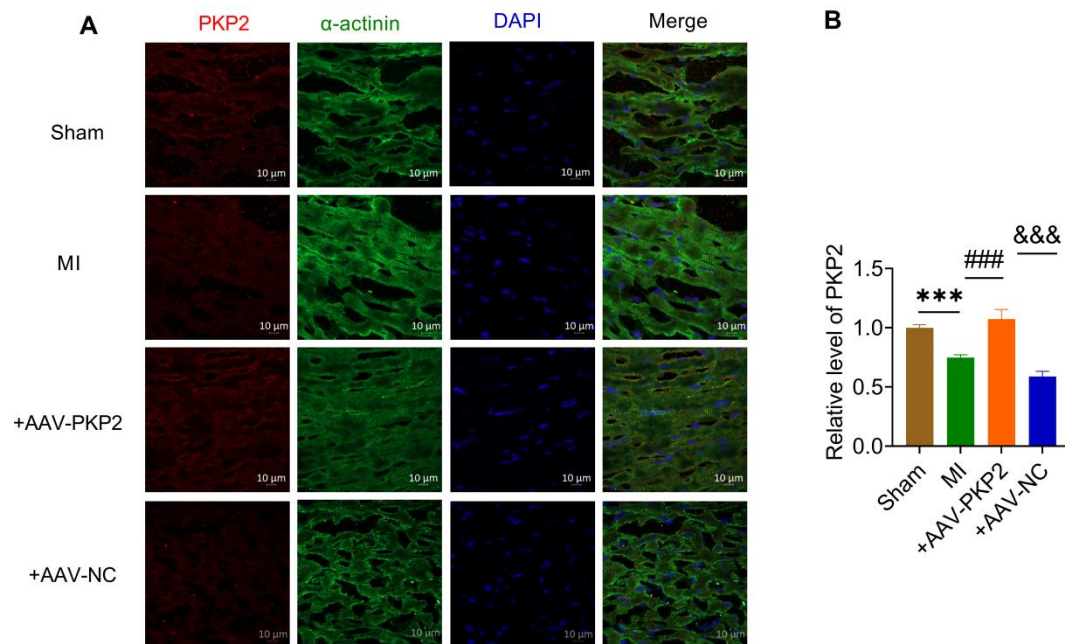


Figure S15. Expression of PKP2 was detected by immunofluorescence. Related to Figure 5.

(A) Representative graph of immunofluorescence results. (B) The expression level of PKP2 in atrial tissue of mice overexpressing PKP2 was detected by immunofluorescence. (Sham $n = 24$, MI $n = 18$, +AAV-PKP2 $n = 9$, +AAV-NC $n = 9$ visions). Red represents PKP2, green represents α -actinin, and blue represents the nucleus. Data are presented as mean \pm SEM. *** $P < 0.001$. ### $P < 0.001$. &&& $P < 0.001$ (One-way ANOVA).

Figure S16

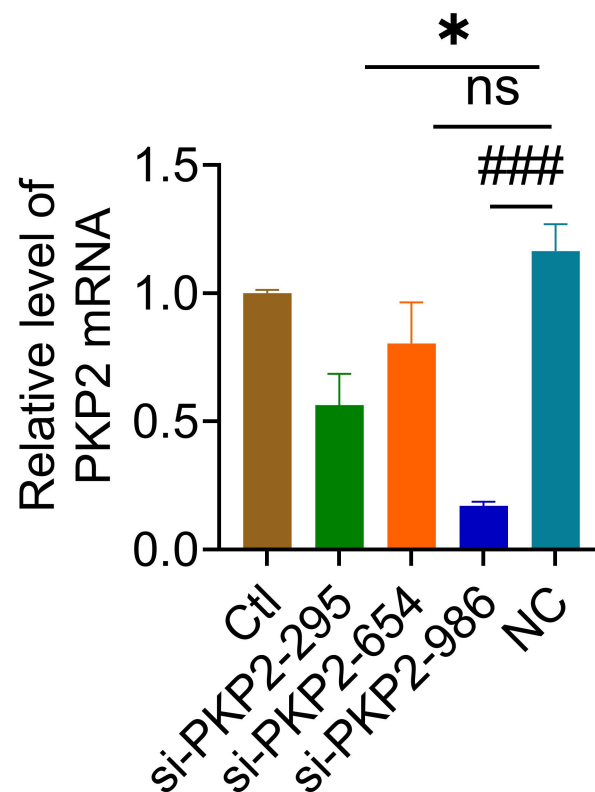


Figure S16. Screening and efficiency verification of si-PKP2 sequences. Related to Figure 7.

The sequences of si-PKP2-295, 654 and 986 were constructed, and the knockdown of PKP2 was detected by Real-time PCR. The efficiency of si-PKP2-986 was the highest (Ctl, si-PKP2-654, si-PKP2-986, NC $n = 4/\text{group}$, si-PKP2-295 $n = 3/\text{group}$). Data are presented as mean \pm SEM. $*P < 0.05$. $###P < 0.001$ (One-way ANOVA).

Figure S17

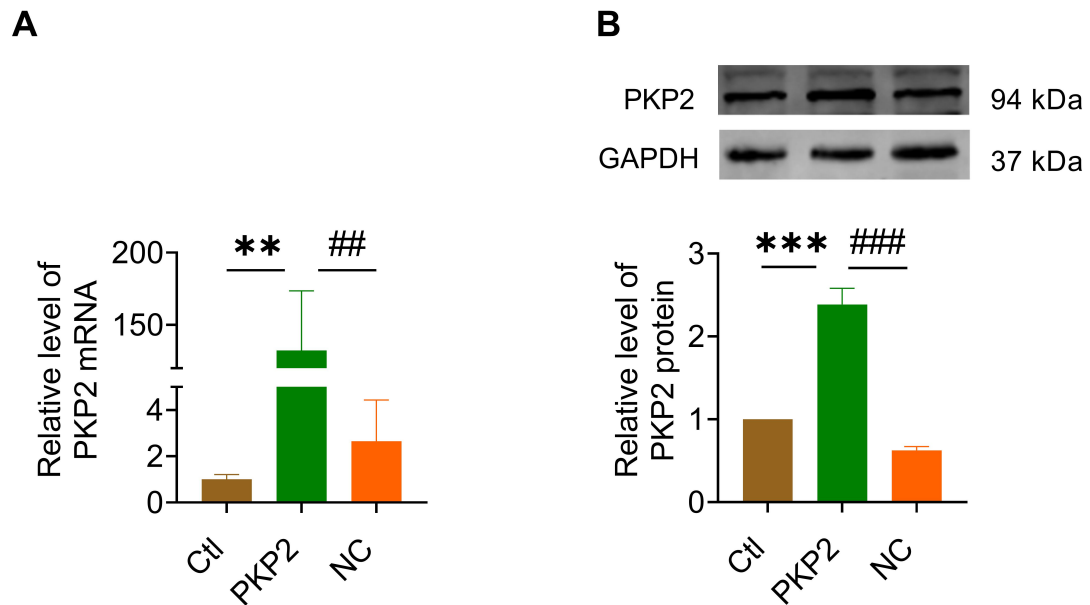


Figure S17. Efficiency verification of PKP2 overexpression plasmid. Related to Figure 8.

(A) Real-time PCR was used to detect the expression of PKP2 in atrial cardiomyocytes ($n = 12/\text{group}$). (B) PKP2 overexpression plasmid was transfected into atrial cardiomyocytes, and the expression efficiency of the plasmid was verified by Western blot ($n = 3/\text{group}$). Data are presented as mean \pm SEM. $**P < 0.01$, and $***P < 0.001$. $##P < 0.01$, and $###P < 0.001$ (One-way ANOVA).

Figure S18

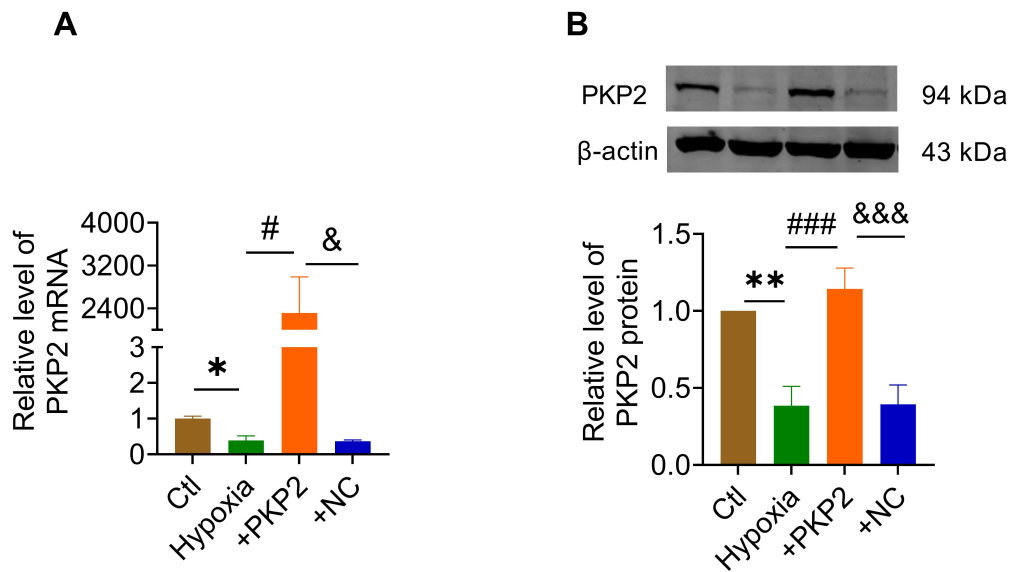


Figure S18. Expression of PKP2 in atrial cardiomyocytes after hypoxia. Related to Figure 8.

(A) Real-time PCR was used to detect the expression of PKP2 in atrial cardiomyocytes (Ctl $n = 3$ /group, Hypoxia, +PKP2, +NC $n = 4$ /group). +PKP2: Hypoxia+PKP2, +NC: Hypoxia+NC. (B) Western Blot results showed that the expression of PKP2 decreased after hypoxia. Compared with +NC group, PKP2 overexpression plasmid could reduce the loss of PKP2 ($n = 5$ /group). Data are presented as mean \pm SEM. * $P < 0.05$. ** $P < 0.01$. # $P < 0.05$, ### $P < 0.001$. & $P < 0.05$, &&& $P < 0.001$ (One-way ANOVA).

Table S1

sequence	
si-MYZAP	CCATCGAAGAGGCCAATAA
si-PKP2	Forward Primer: 5'-GCAGACCAUGUACCAGUAUTT-3'
	Reverse Primer: 5'-AUACUGGUACAUGGUCUGCTT-3'

Table S1. si-MYZAP and si-PKP2 knock-down sequences used in the experiment. Related to Figure 4 and 7.

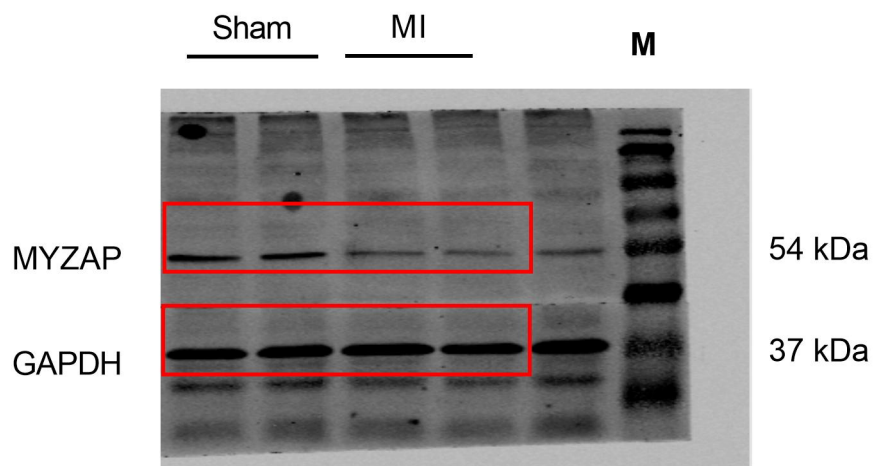
Table S2

Primer sequence	
CCRR	Forward Primer: 5'-GTGCTGCCATCGAAAAATCTG-3'
	Reverse Primer: 5'-CTCCCCAGACTCAATGCTTC-3'
MYZAP	Forward Primer: 5'-TGAGGAGAAACTGCAGGAGG-3'
	Reverse Primer: 5'-CGTTCAATCAGCCTGTCCAG-3'
PKP2	Forward Primer: 5'-GCAGCTTGTTGGAAGAGACC-3'
	Reverse Primer: 5'-CTACTGCGGACTGAGCTCCT-3'
TLR2	Forward Primer: 5'-ACGAGCAAGATCAACAGGAGA-3'
	Reverse Primer: 5'-CTTCCTGAATTTGTCCAGTACA-3'
TLR4	Forward Primer: 5'-TGGTTCCTGGAACACCAAA-3'
	Reverse Primer: 5'-AGCAAGGGTCGAAGTTAGCA-3'
Nav1.5	Forward Primer: 5'-GAAGGAACGCAGCACAGACAG-3'
	Reverse Primer: 5'-CATCGCCCTTGACCCATACTA-3'
IL-6	Forward Primer: 5'-CTCCCAACAGACCTGTCTATAC-3'
	Reverse Primer: 5'-CCATTGCACAACCTTTTTCTCA-3'
IL-1 β	Forward Primer: 5'-CTACAGGCTCCGAGATGAACAAC-3'
	Reverse Primer: 5'-TCCATTGAGGTGGAGAGCTTTC-3'
TNF- α	Forward Primer: 5'-ATCCGCGACGTGGAAGTGG-3'
	Reverse Primer: 5'-ACCGCCTGGAGTTCTGGAA-3'
MCP1	Forward Primer: 5'-AAGATGATCCCAATGAGTAGGC-3'
	Reverse Primer: 5'-AGGTGGTTGTGGAAAAGGTAGT-3'
GAPDH	Forward Primer: 5'-AAGAAGGTGGTGAAGCAGGC-3'
	Reverse Primer: 5'-TCCACCACCCAGTTGCTGTA-3'

Table S2. qRT-PCR primer sequence used in the experiment. Related to Figure 1,2,3,4,7 and 8.

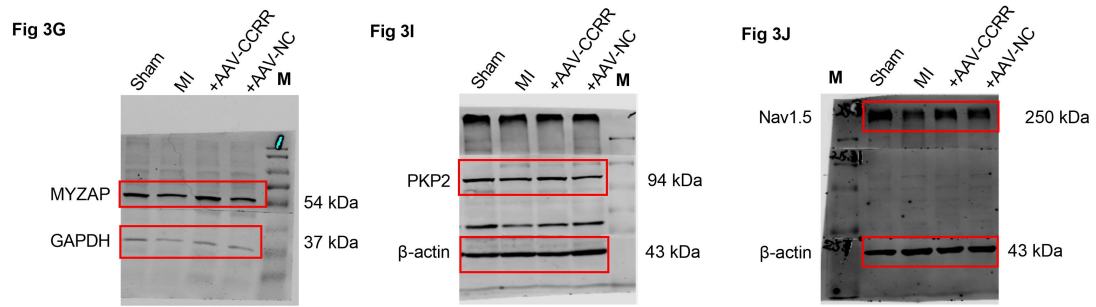
Data S1

Fig 1J



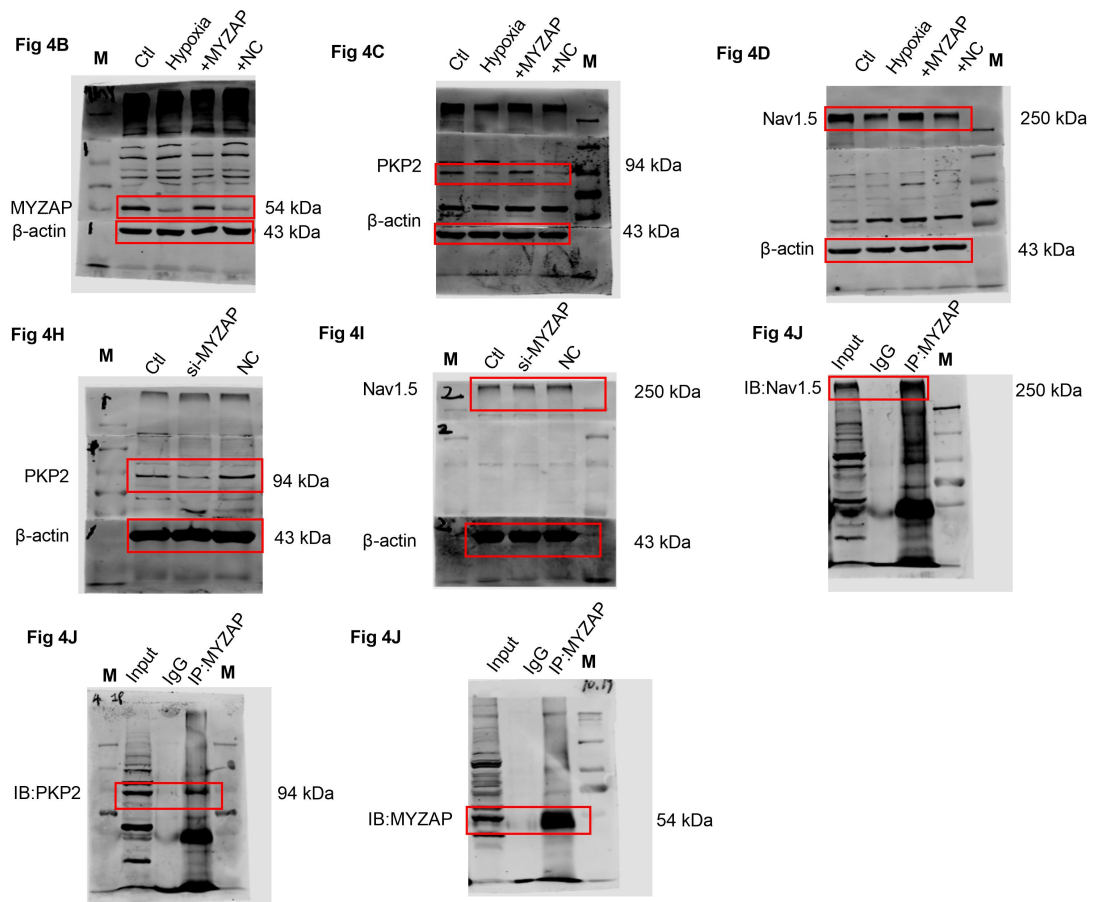
Data S1. The expression of CCRR and MYZAP in atrial tissue decreased after MI. Related to Figure 1.

Data S2



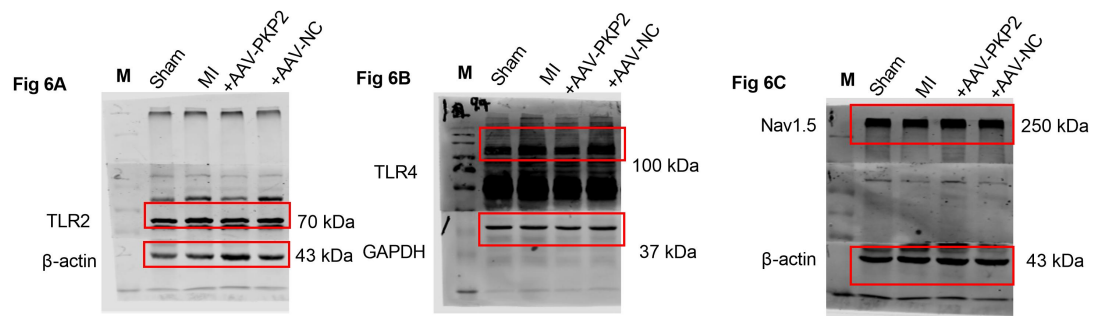
Data S2. CCR reduces the incidence and duration of AF, and improves atrial conduction in mice with MI. Related to Figure 3.

Data S3



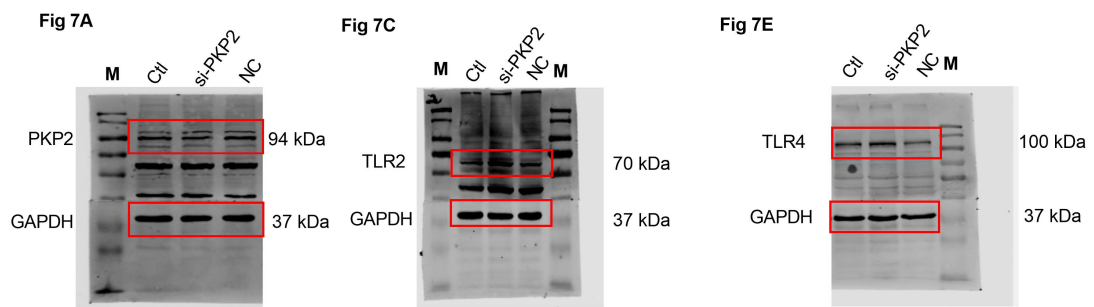
Data S3. CCR2 regulates the expression of MYZAP, PKP2 and Nav1.5. Related to Figure 4.

Data S4



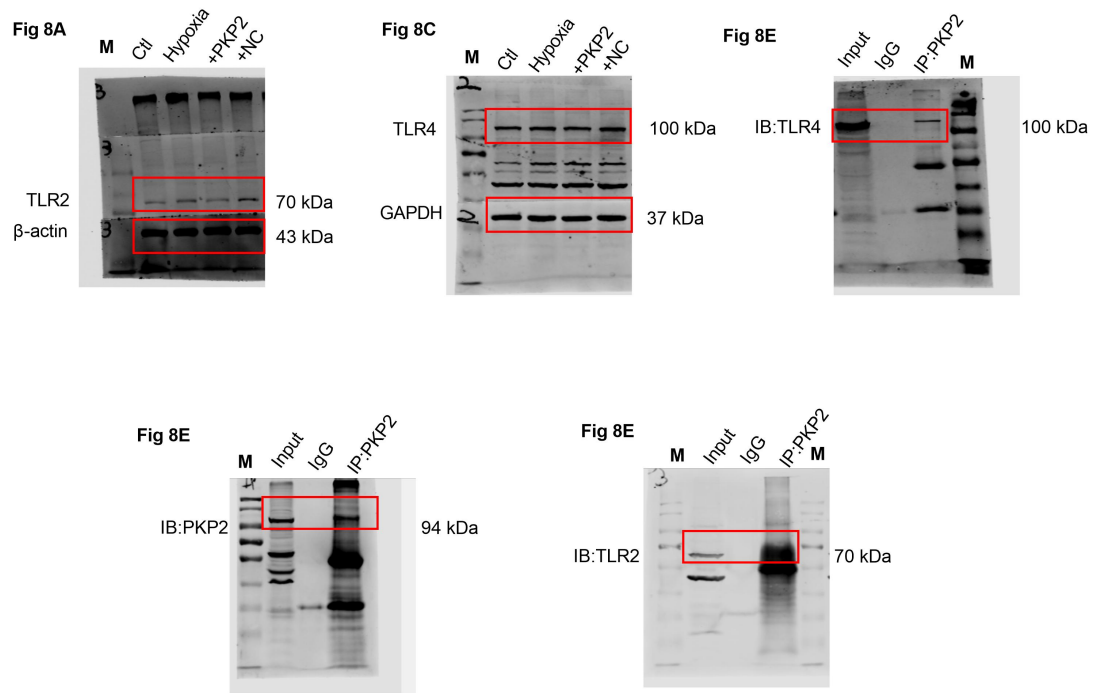
Data S4. PKP2 is an upstream regulator of TLR2/TLR4/Nav1.5. Related to Figure 6.

Data S5



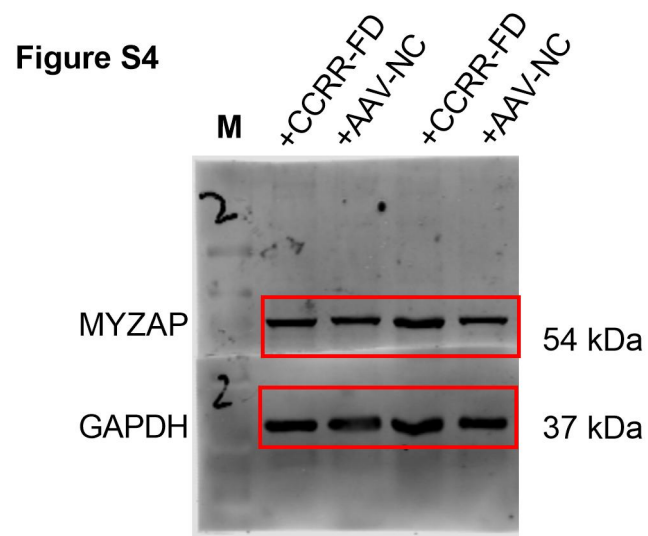
Data S5. Knockdown of PKP2 enhances inflammation after MI via TLR2/TLR4/Nav1.5 pathway. Related to Figure 7.

Data S6



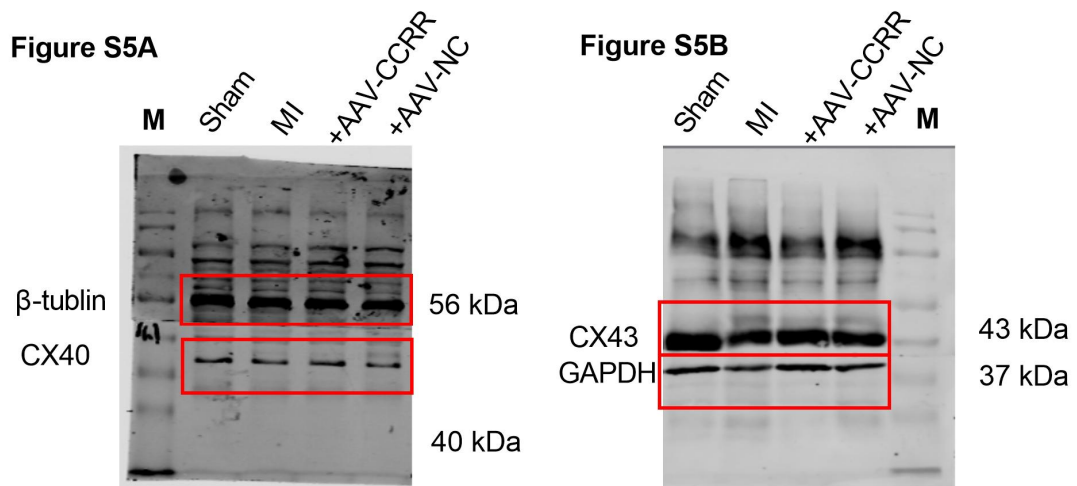
Data S6. PKP2 alleviates inflammatory response after MI by regulating the TLR2/TLR4/Nav1.5 pathway. Related to Figure 8.

Data S7



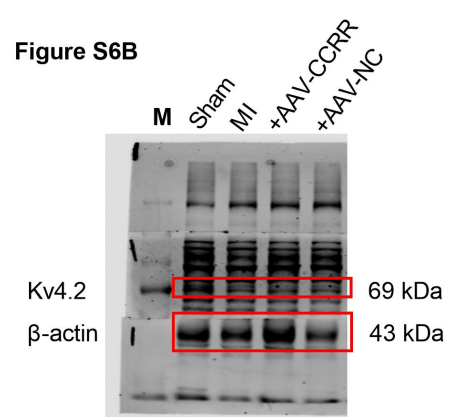
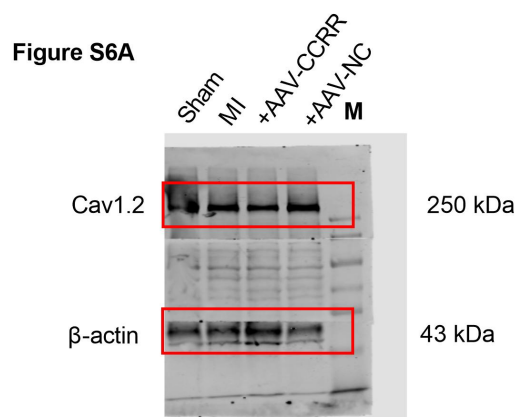
Data S7. CCRR-Functional domain (CCRR-FD) reverses the down-regulation of MYZAP expression in atrial tissue after MI. Related to Figure S4.

Data S8



Data S8. Overexpression of CCRR reverses the decreased expression of MYZAP after hypoxia. Related to Figure S5.

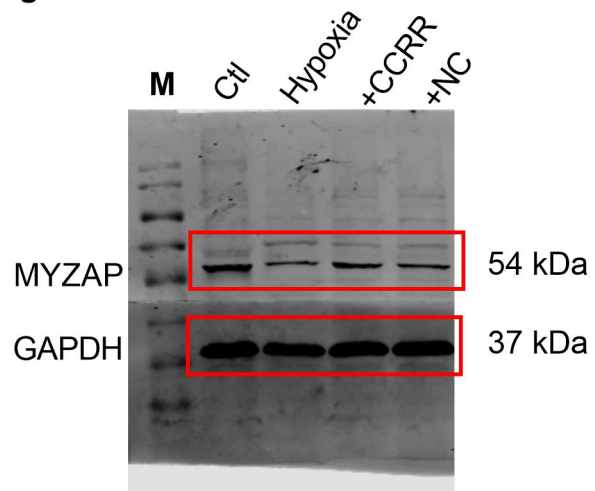
Data S9



Data S9. CCRR may act as an upstream regulator to regulate the expression of PKP2 and Nav1.5. Related to Figure S6.

Data S10

Figure S8B



Data S10. Overexpression of CCRR reverses the decreased expression of MYZAP after hypoxia. Related to Figure S8.

Data S11

Figure S9A

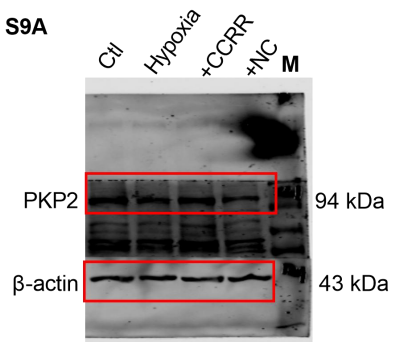
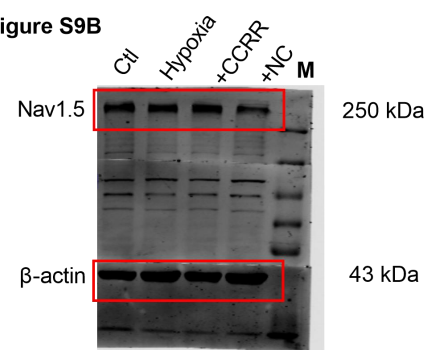


Figure S9B



Data S11. CCR may act as an upstream regulator to regulate the expression of PKP2 and Nav1.5. Related to Figure S9.

Data S12

Figure S10A

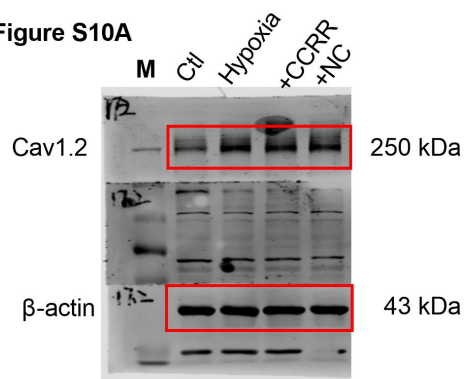
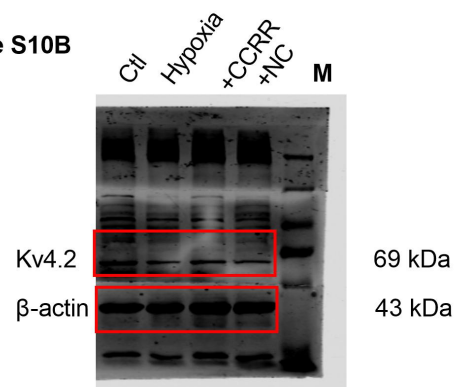
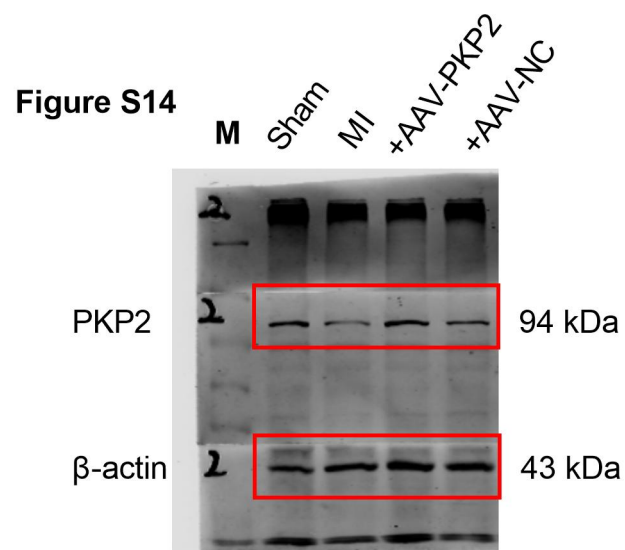


Figure S10B



Data S12. CCRR did not significantly regulate the expression levels of Cav1.2 and Kv4.2 in hypoxic atrial myocytes. Related to Figure S10.

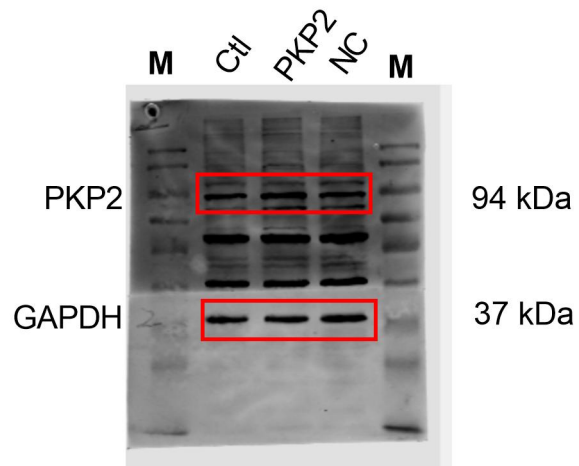
Data S13



Data S13. Efficiency verification of overexpressing AAV-PKP2 virus. Related to Figure S14.

Data S14

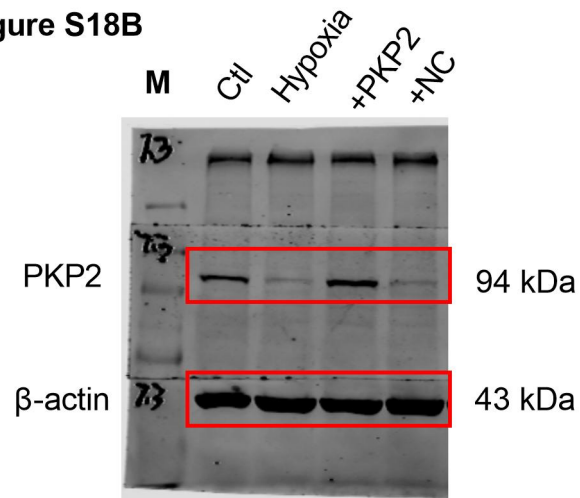
Figure S17B



Data S14. Efficiency verification of PKP2 overexpression plasmid. Related to Figure S17.

Data S15

Figure S18B



Data S15. Expression of PKP2 in atrial cardiomyocytes after hypoxia. Related to Figure S18.